

# Light and Electron Microscopy Study of Glycogen Synthase Kinase-3 $\beta$ in the Mouse Brain

Emma Perez-Costas<sup>1</sup>, Johanna C. Gandy<sup>1</sup>, Miguel Melendez-Ferro, Rosalinda C. Roberts, Gautam N. Bijur\*

Department of Psychiatry and Behavioral Neurobiology, University of Alabama at Birmingham, Birmingham, Alabama, United States of America

## Abstract

Glycogen synthase kinase-3 $\beta$  (GSK3 $\beta$ ) is highly abundant in the brain. Various biochemical analyses have indicated that GSK3 $\beta$  is localized to different intracellular compartments within brain cells. However, ultrastructural visualization of this kinase in various brain regions and in different brain cell types has not been reported. The goal of the present study was to examine GSK3 $\beta$  distribution and subcellular localization in the brain using immunohistochemistry combined with light and electron microscopy. Initial examination by light microscopy revealed that GSK3 $\beta$  is expressed in brain neurons and their dendrites throughout all the rostrocaudal extent of the adult mouse brain, and abundant GSK3 $\beta$  staining was found in the cortex, hippocampus, basal ganglia, the cerebellum, and some brainstem nuclei. Examination by transmission electron microscopy revealed highly specific subcellular localization of GSK3 $\beta$  in neurons and astrocytes. At the subcellular level, GSK3 $\beta$  was present in the rough endoplasmic reticulum, free ribosomes, and mitochondria of neurons and astrocytes. In addition GSK3 $\beta$  was also present in dendrites and dendritic spines, with some postsynaptic densities clearly labeled for GSK3 $\beta$ . Phosphorylation at serine-9 of GSK3 $\beta$  (pSer9GSK3 $\beta$ ) reduces kinase activity. pSer9GSK3 $\beta$  labeling was present in all brain regions, but the pattern of staining was clearly different, with an abundance of labeling in microglia cells in all regions analyzed and much less neuronal staining in the subcortical regions. At the subcellular level pSer9GSK3 $\beta$  labeling was located in the endoplasmic reticulum, free ribosomes and in some of the nuclei. Overall, in normal brains constitutively active GSK3 $\beta$  is predominantly present in neurons while pSer9GSK3 $\beta$  is more evident in resting microglia cells. This visual assessment of GSK3 $\beta$  localization within the subcellular structures of various brain cells may help in understanding the diverse role of GSK3 $\beta$  signaling in the brain.

**Citation:** Perez-Costas E, Gandy JC, Melendez-Ferro M, Roberts RC, Bijur GN (2010) Light and Electron Microscopy Study of Glycogen Synthase Kinase-3 $\beta$  in the Mouse Brain. PLoS ONE 5(1): e8911. doi:10.1371/journal.pone.0008911

**Editor:** Cheng-Xin Gong, New York State Institute for Basic Research, United States of America

**Received:** July 7, 2009; **Accepted:** January 5, 2010; **Published:** January 27, 2010

**Copyright:** © 2010 Perez-Costas et al. This is an open-access article distributed under the terms of the Creative Commons Attribution License, which permits unrestricted use, distribution, and reproduction in any medium, provided the original author and source are credited.

**Funding:** This work was supported by National Institutes of Health (NIH) grants NS044853 to GNB, MH66123 and MH60744 to RCR, and the University of Alabama at Birmingham Neuroscience Core grant NS47466. JCG is supported by the Cellular and Molecular Biology Program training grant GM008111 and the Civitan International Research Center Emerging Scholars Award. The funders had no role in study design, data collection and analysis, decision to publish, or preparation of the manuscript.

**Competing Interests:** The authors have declared that no competing interests exist.

\* E-mail: gautam@uab.edu

These authors contributed equally to this work.

## Introduction

Glycogen synthase kinase-3 $\beta$  (GSK3 $\beta$ ) is a ubiquitous enzyme which is found in nearly all mammalian tissues. However, it is highly abundant in the brain [1]. GSK3 $\beta$  was originally shown to phosphorylate and inhibit glycogen synthase. However, the last decade has witnessed a resurgent interest in this enzyme because it has been shown to be dysregulated in numerous pathologies. Much attention has been focused on GSK3 $\beta$  signaling in the brain due to its involvement in neurologic and psychiatric diseases. For example, unregulated GSK3 $\beta$  activity appears to underlie the pathogenesis of Alzheimer's disease [2–5], Parkinson's disease [6,7], and Huntington's disease [8]. In addition, anomalous GSK3 $\beta$  signaling has been reported in psychiatric diseases, including bipolar disorder [9,10] and schizophrenia [11,12]. Due to its involvement in many brain disorders, it has become apparent that normal GSK3 $\beta$  signaling is necessary to maintain brain homeostasis.

The overall levels of GSK3 $\beta$  in the normal adult brain rarely appear to fluctuate, and nearly all brain regions have been shown

to have high levels of GSK3 $\beta$ , although there are marked regional differences of GSK3 $\beta$  mRNA levels in the human brain [13]. However, during development the levels of GSK3 $\beta$  in the brain do change, with the level of expression peaking during embryonic development. In addition, previous investigations have shown that in post-mortem tissues from individuals with schizophrenia the levels of GSK3 $\beta$  are decreased [11]. In addition, GSK3 $\beta$  activity is also dependent on its phosphorylation status. GSK3 $\beta$  is constitutively active, but phosphorylation at its serine-9 site decreases its activity. Several therapeutic drugs have been shown to increase GSK3 $\beta$  serine-9 phosphorylation and inhibit its activity, such as lithium [9,14] and pilocarpine [15], as well as a host of other agents such as growth factors, neurotransmitters, cytokines, anesthetics, and hormones [16,17]. Thus, the anatomical distribution of GSK3 $\beta$  in different brain regions, its overall levels, and the phosphorylation status at serine-9 of GSK3 $\beta$  likely all affect its physiological actions.

GSK3 $\beta$  is also involved in numerous signaling cascades which can impact many biochemical processes, thus its activity must be finely regulated. In fact, the regulation of GSK3 $\beta$  is multi-tiered.

As already mentioned, GSK3 $\beta$  is inhibited by its phosphorylation at its Ser9 site. Its association with other proteins, such as those of the Wnt signaling pathway, can also affect GSK3 $\beta$  activity [18,19]. Furthermore, it was shown that GSK3 $\beta$  activity is dependent on its subcellular distribution [20]. GSK3 $\beta$  has been reported to exist in the cytosol [21], the nucleus [22], and the mitochondria [23,24]. Thus, intracellular localization can affect the activity of GSK3 $\beta$  because it dictates its accessibility to various cell compartment-specific substrates. Interestingly, very little is known about the intracellular distribution of GSK3 $\beta$  in the brain.

Although there are studies which have investigated the neuroanatomical distribution of GSK3 $\beta$  in the brain by light microscopy [4,5,25–31], nearly nothing has been described about GSK3 $\beta$  visual localization in the brain at the ultrastructural level. Using immunohistochemistry for the detection of GSK3 $\beta$  and phospho-serine-9 GSK3 $\beta$  in combination with light microscopy and transmission electron microscopy, we show the differential expression of GSK3 $\beta$  and phospho-serine-9 GSK3 $\beta$  within different brain regions and their intracellular distribution within different subcellular compartments.

## Materials and Methods

### Ethics Statement

All animal housing, care, and experimental procedures were done in accordance with, and approved by, the University of Alabama at Birmingham Institutional Animal Care and Use Committee (IACUC) guidelines. Mice were euthanized according to an approved IACUC protocol.

### Immunohistochemistry

Six adult male C57BL6 mice (10 to 12 week old) were used in this study. Mice were euthanized by decapitation and the brains were immediately removed, quickly rinsed in cold 0.1M phosphate buffer (PB), and fixed by immersion in a 4% paraformaldehyde and 0.1% glutaraldehyde in PB solution, pH 7.4, at 4°C overnight. The brains were then sectioned in the coronal plane on a vibratome and 40  $\mu$ m free-floating sections were obtained. The sections were kept in PB at 4°C until processed for immunohistochemistry.

For the immunohistochemical localization of GSK3 $\beta$  and phospho-serine-9 GSK3 $\beta$  (pSer9GSK3 $\beta$ ) free-floating sections were rinsed in phosphate buffered saline (PBS), quenched in 1% sodium borohydride in PBS for 15 minutes, rinsed multiples times in PBS, and the endogenous peroxidase was blocked in a solution of 1.5% hydrogen peroxide in PBS for five minutes. After rinsing in PBS, non-specific binding sites in the sections were blocked with 2% normal goat serum in PBS for 30 minutes. The sections were then incubated for 72 hours at 4°C in a 1:500 dilution of a monoclonal rabbit GSK3 $\beta$  antibody, or a 1:100 dilution of a polyclonal rabbit pSer9GSK3 $\beta$  antibody (Cell Signaling, Danvers, MA). For the GSK3 $\beta$  antibody two types of controls were performed: some sections were incubated in the absence of primary antibody, while others were incubated with the GSK3 $\beta$  antibody pre-adsorbed with two micrograms of GSK3 $\beta$  blocking peptide (Cell Signaling). For the pSer9GSK3 $\beta$  antibody the immunohistochemical controls consisted of sections incubated in the absence of the primary antibody. After rinsing in PBS, all sections were incubated with a biotinylated goat anti-rabbit secondary antibody (Vector laboratories, Burlingame, CA) diluted 1:200 for 1 h at room temperature. Then, sections were rinsed in PBS and incubated for 30 minutes with an avidin-biotinylated horseradish peroxidase complex (Vectastain ABC system, Vector Laboratories). After rinsing in PBS, the sections were developed in

a diaminobenzidine solution (10 mg/15 ml PBS; Sigma, St Louis, MO) containing 0.03% hydrogen peroxide for 2–5 min to visualize the reaction product. The sections were then rinsed in PB and processed for light or electron microscopy.

### Light Microscopy

Immunostained sections were mounted on Colorfrost/Plus slides (Fisher, Pittsburgh, PA), air-dried overnight, dehydrated in ascending series of ethanol, cleared in xylene and coverslipped with Eukitt mounting media (O. Kindler, Germany). Sections were viewed and photographed using a Nikon DS-Fi1 color digital camera coupled to a Nikon Eclipse 50i. Images were converted to grey scale and adjusted for brightness and contrast using Corel PhotoPaint 12 (Corel Corporation, Ottawa, Canada). Photomontage and lettering were done using CorelDraw 12.

### Electron Microscopy

Immunostained sections were rinsed in PB and immersed in a solution of 1% osmium tetroxide in PB for 1 hour, then rinsed in PB and gradually dehydrated on series of ethanol from 30% to 70%. After that, the sections were stained with a solution of 1% uranyl acetate in 70% ethanol for 1 hour and further dehydrated in ethanol. After dehydration was completed the sections were cleared in propylene oxide and infiltrated with Epon resin overnight at room temperature. The following day the sections were flat-embedded in new Epon resin and allowed to polymerize in an oven at 60°C for 72 hours. Selection of regions of interest for electron microscopy was performed by visualizing the flat-embedded sections on a Nikon Eclipse 50i light microscope, carefully identifying anatomical regions and re-dissecting these regions for ultramicrotomy. Ultrathin sections (90 nm thick) were obtained using a Leica EM UC6 ultramicrotome (Leica Microsystems, Wetzlar, Germany), mounted on copper grids and observed and photographed using a Hitachi TEM model H-7650-II (Hitachi, Japan) equipped with an AMT digital camera (Danvers, MA). Photomontage and lettering was done as for light microscopy.

### Western-Blot

For pSer9GSK3 $\beta$  antibody staining controls only, mouse brain homogenates from two mice (n = 1 control, n = 1 pilocarpine) were used to test the specificity of the antibodies used in the study. Western blot assays were first performed for both GSK3 $\beta$  and GSK3 $\alpha$ . In addition, to confirm the specificity of the pSer9GSK3 $\beta$  antibody, serine-9 phosphorylation of GSK3 $\beta$  in the mouse brain was induced by the intraperitoneal injection of pilocarpine (30 mg/kg body weight) diluted in saline [15]. After 15 minutes, brains were dissected and homogenates were obtained and immunoblotted with both pSer9GSK3 $\beta$  and GSK3 $\beta$  antibodies.

## Results

In the present study, we focused on the neuroanatomical and intracellular distribution of GSK3 $\beta$  in the adult mouse brain using immunohistochemistry for the detection of GSK3 $\beta$  in combination with light and electron microscopy. We first performed a light microscopy study of the distribution of GSK3 $\beta$  in the adult mouse brain to compare with previous studies published on the distribution of GSK3 $\beta$  in other rodent species. After studying the distribution and subcellular localization of the constitutively active GSK3 $\beta$ , we proceeded to analyze the distribution and subcellular localization of the inhibited form of GSK3 $\beta$  in the brain by using a specific antibody against pSer9GSK3 $\beta$  at the light and electron microscopy level.

### Light Microscopy Analysis of GSK3 $\beta$ Immunohistochemistry in the Adult Mouse Brain

It was initially necessary to confirm the specificity of the phospho-independent GSK3 $\beta$  antibody (Cell Signaling, catalog # 9315) used for this study. The GSK3 $\beta$  antibody was first used to immunoblot mouse brain lysates (Figure 1A). As a further test of specificity the antibody was also mixed with another separate antibody for GSK3 $\alpha$  (Cell Signaling, catalog #9338). Then, the mixture of the two antibodies was incubated with a GSK3 $\beta$  blocking peptide (Cell Signaling, catalog #1073) to specifically bind to the GSK3 $\beta$  antibody and block it. This mixture was then used to immunoblot the brain lysates (Figure 1A). Our results show that the GSK3 $\beta$  antibody is specifically blocked by the peptide while GSK3 $\alpha$  is not blocked by this peptide. In addition, when brain lysates were immunoblotted with the GSK3 $\beta$  antibody alone, only the one GSK3 $\beta$  protein band was evident on the autoradiography film, further indicating that this antibody does not recognize other proteins. As further tests of antibody

specificity, immunostaining was performed in parallel sections of the mouse brain to compare the staining obtained with the GSK3 $\beta$  antibody alone, preadsorption of GSK3 $\beta$  with the blocking peptide, and omission of the primary antibody. Our results showed that GSK3 $\beta$  strongly labels neurons in the cortex and striatum (see pSer9GSK3 $\beta$  results and figures) whereas in an adjacent section that was processed with the peptide-preadsorbed antibody no immunostaining was observed (Figure 1C). Additionally, incubation with a non-specific rabbit IgG, or omission of the primary antibody produced no staining (data not shown). Together these results confirmed the specificity of GSK3 $\beta$  immunolabeling and validated the use of this antibody for our studies at the light and electron microscope.

Our study commenced with a light microscopic examination of the phospho-independent GSK3 $\beta$  immunohistochemical labeling in adult male C57BL6 mouse brain. The most salient feature under light microscopy was the abundance of GSK3 $\beta$  immunoreactivity in neuronal populations throughout multiple brain

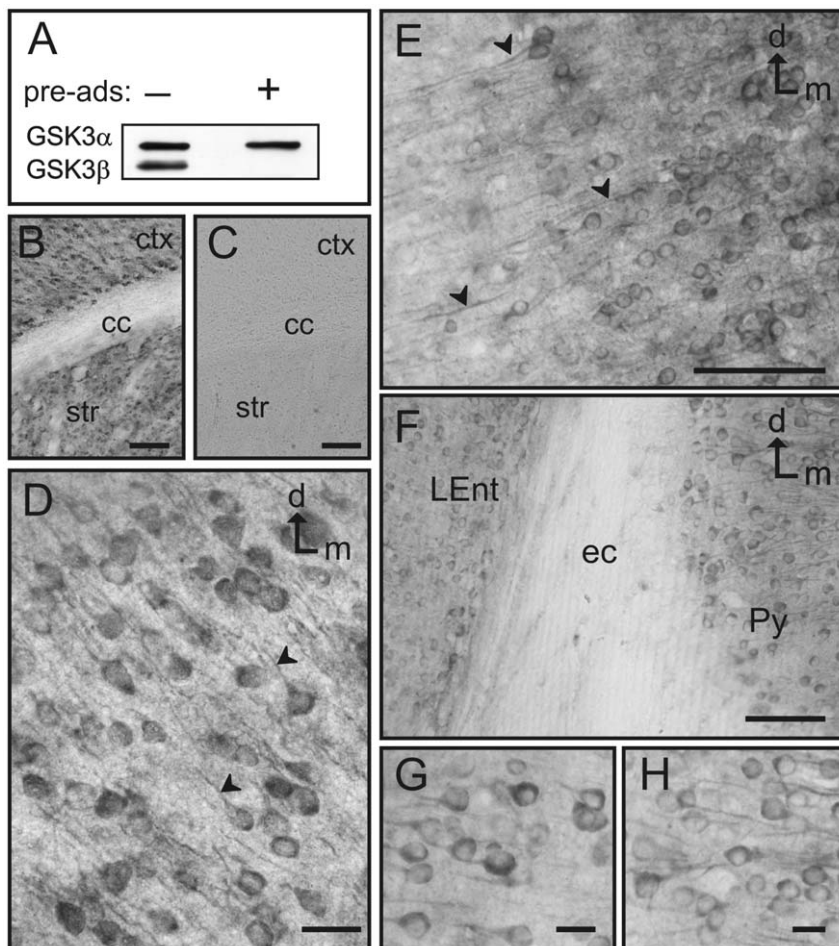


**Figure 1. GSK3 $\beta$  specificity and distribution in the cortex.** **A)** Immunoblot of mouse brain lysates showing the specificity of the antibody used. The left column shows the presence of 2 bands, an upper band (GSK3 $\alpha$ ) and a lower band (GSK3 $\beta$ ), when there is no blocking peptide present (–). However, in the presence of the GSK3 $\beta$  blocking peptide (+), the lower GSK3 $\beta$  band is specifically blocked while the upper GSK3 $\alpha$  band is still present. **B–C)** Immunohistochemistry specificity: GSK3 $\beta$  immunostaining (**B**) displays robust labeling in the cortex (ctx) and striatum (str), while there is no staining in the corpus callosum (cc). Addition of the blocking peptide (**C**) produces complete abolition of the staining in these same regions. **D)** GSK3 $\beta$  immunolabeling in the primary somatosensory cortex. Neuronal cytoplasm and the initial segment of the apical dendrites is strongly immunolabeled (arrowheads). **E)** GSK3 $\beta$  blocking peptide (+), the piriform cortex also show clearly stained processes running laterally (arrowheads). **F)** Image showing GSK3 $\beta$ -labeled neurons in the lateral entorhinal cortex (LEnt) and the pyramidal cell layer of the hippocampus (Py) separated by the unlabeled external capsule (ec). **G–H)** Detail of labeled neurons in the lateral entorhinal cortex (**G**) and pyramidal cell layer of the hippocampus (**H**). [d: dorsal; m: medial; Scale bars: 100  $\mu$ m in B–C; 25  $\mu$ m in E–F; 5  $\mu$ m in D and G–H] doi:10.1371/journal.pone.0008911.g001

regions. The paucity, but not a complete lack, of glial GSK3 $\beta$  staining contrasted with the copious labeling of neuronal cells within most neuronal subtypes and cell layers within the cortex and hippocampus, as well as in many other brain regions. In the following paragraphs we will describe the more salient features of GSK3 $\beta$  distribution across the rostrocaudal extent of the adult mouse brain.

In the cortex GSK3 $\beta$  is abundantly present from the most rostral to the most caudal cortical areas. Many areas of the cortex present immunolabeled cell bodies, but also clearly immunostained processes, especially in the dorsal areas of the motor cortex, dorso-lateral areas corresponding with the somatosensory cortex (Figure 1D), and in the piriform cortex (Figure 1E). In some areas such as the motor cortex, evident differences in staining intensity were observed across the different cortical layers, with the areas corresponding with layers I, III and V-VI showing more intense labeling. A similar labeling pattern can also be seen in the cells of the entorhinal cortex and the pyramidal cell layer of the hippocampus (Figures 1F-H).

Throughout the hippocampus GSK3 $\beta$  immunoreactivity was evident at low magnification with staining differences among hippocampal layers (Figure 2A). The pyramidal neurons in the cornu ammonis (CA) and the polymorphic layer of the dentate gyrus exhibited particularly high levels of staining that contrast with the lack of staining in adjacent areas such as the molecular layer (Figure 2A). At higher magnification, the polymorphic layer of the dentate gyrus contained high levels of GSK3 $\beta$  in both the cell body and in the initial segment of processes (Figure 2B). Also, closer inspection of labeling in the CA1 region (Figure 2C) reveals multiple pyramidal neurons with high levels of GSK3 $\beta$  in both the cell body and the dendrites. The most robust immunostaining of

the CA regions was apparent in the CA3, which again contained high somatic and dendritic staining of GSK3 $\beta$  in numerous pyramidal neurons (Figure 2D).

Other areas of the brain also presented prominent GSK3 $\beta$  labeling, especially the striatum, the globus pallidus, thalamus, the substantia nigra and some brainstem areas (Figure 3). In contrast, hypothalamic nuclei presented less robust immunolabeling (not shown). Within the striatum GSK3 $\beta$  labeling is prominently present in cell bodies but not in the numerous fiber bundles that cross this area of the brain (Figure 3A). Although striatal fiber bundles and the corpus callosum are prominently unlabeled, some scattered immunolabeled small cells are observed in some areas of the corpus callosum, probably corresponding with glial cells. Prominently labeled neurons are also observed in the globus pallidus (not shown). Caudal to the striatum, the thalamic region presents several strongly labeled nuclei, including the reticular and geniculate nuclei (Figure 3B). The subthalamic nucleus is also strongly labeled (Figure 3C) while adjacent hypothalamic areas present only weakly labeled neurons. In the midbrain, the substantia nigra and ventral tegmental area present GSK3 $\beta$  positive neurons, the substantia nigra *pars compacta* being the most strongly labeled area (Figure 3D). Also in this area, neurons of the red nucleus are prominently labeled (Figure 3E). Finally, the cerebellum presents layer specific immunolabeling; the granular layer was virtually devoid of immunostaining, while the Purkinje cell layer presents clusters of GSK3 $\beta$ -labeled neurons interspersed with other clusters of unlabeled neurons. The molecular layer is also labeled and some strongly stained Purkinje cell dendrites are clearly seen (Figure 3F). Thus, high levels of GSK3 $\beta$  labeling were found in all the brain regions examined. Furthermore, this evaluation by light microscopy placed into context the subcellular

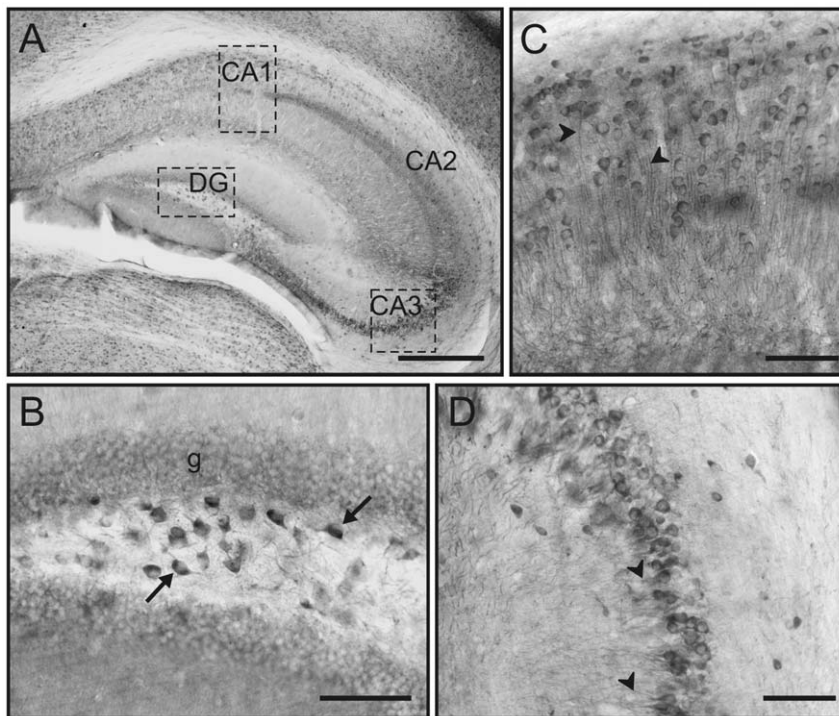


**Figure 2. GSK3 $\beta$  labeling in the hippocampus.** **A)** Low magnification image showing GSK3 $\beta$  labeling in different layers of the hippocampus. This immunolabeling is especially robust in the Cornu Amonis (CA) subfields and in the dentate gyrus (DG). **B)** Detail of the dentate gyrus showing labeling in the neurons of the polymorphic layer (arrows) and also in the granular layer (g). **C–D)** Detail of GSK3 $\beta$  immunolabeling in pyramidal cells of CA1 (**C**) and CA3 (**D**) and in their processes (arrowheads). [Scale bars: 400  $\mu$ m in A; 100  $\mu$ m in B–D]

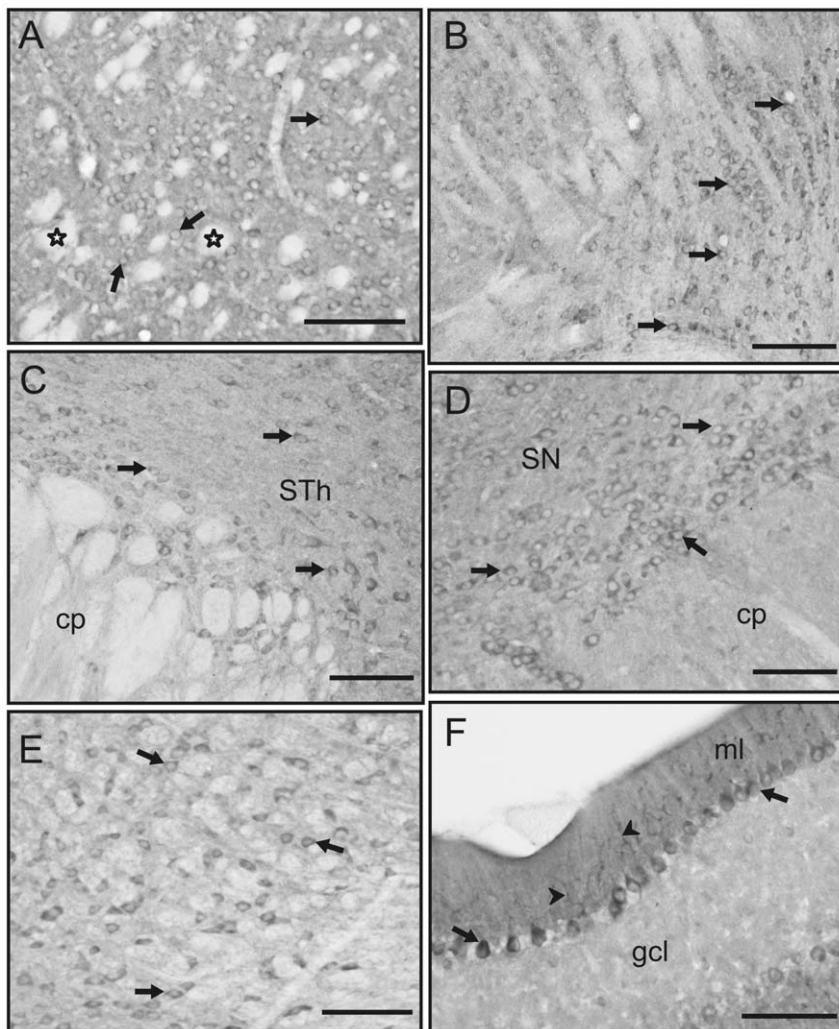


**Figure 3. GSK3 $\beta$  labeling in subcortical regions and in the cerebellum.** **A**) GSK3 $\beta$ -labeled neurons in the striatum (arrows). Note that fiber bundles crossing this area are devoid of immunolabeling (outlined stars). **B–E**) Labeled neurons (arrows) in the geniculate nucleus of the thalamus (**B**) appear in “rows” strongly immunostained with clear nucleus and almost no processes visible. In the subthalamic nucleus (STh), labeled neurons are surrounded by labeling that may correspond with small processes (**C**). The same type of labeling is observed in the substantia nigra (SN) where neurons present strongly stained cell bodies (**D**). The red nucleus (**E**) shows GSK3 $\beta$  positive neurons (arrows) interspersed with negative fiber bundles. **F**) In the cerebellum, Purkinje cells are GSK3 $\beta$  immunolabeled (arrows). There is strong labeling in the molecular layer (ml), while the granule cell layer (gcl) is almost devoid of staining. Note also that Purkinje cell dendrites in the molecular layer are strongly labeled (arrowheads). [cp: cerebellar peduncle; Scale bars: 50  $\mu$ m in all images] doi:10.1371/journal.pone.0008911.g003

distribution of GSK3 $\beta$  which was examined by electron microscopy.

### Subcellular Localization of GSK3 $\beta$ at the Electron Microscope

Since the pattern of GSK3 $\beta$  labeling at the light microscopic level was similar among the brain regions examined, we selected one region (piriform cortex) to study in more detail at the electron microscopic level (Figures 4A–F, and Figures 5A–E). GSK3 $\beta$  labeling at the ultrastructural level was similar among the several cases that were examined. Consistent with light microscopy, GSK3 $\beta$  labeling was most evident in the soma and the dendritic shafts of neurons (Figure 4F, 5D–E). There did not appear to be differences in the staining pattern of cell bodies based on the morphology of the neuron (pyramidal vs. non-pyramidal). GSK3 $\beta$  labeling was abundant preferentially in the cytoplasm of neuronal somata (Figure 4A–E, 5A–B). Closer inspection of the soma

revealed GSK3 $\beta$  concentrated on ribosomes, rough endoplasmic reticulum (RER), and the outer membranes of mitochondria (Figure 4B–F, 5A–E). Examination of dendritic shafts showed clear labeling of GSK3 $\beta$  throughout the cytoplasm, on ribosomes, and on the outer mitochondrial membrane (Figure 4F, 5C–D). Interestingly, dendritic mitochondria showed more robust GSK3 $\beta$  staining than mitochondria in the neuronal cell body (compare Figure 4E to 4F or 5E). In the neuropil, dense immunolabeling was found in postsynaptic densities in both dendrites and dendritic spines.

In neuronal profiles, labeling was consistently absent from the nucleus, myelinated and unmyelinated axons (Figure 4B, 5C), axon terminals (Figure 4F) and lysosomes (Figure 4B). Interestingly, this phospho-independent GSK3 $\beta$  staining was not evident in the oligodendrocytes, endothelial cells or microglia (Figure 5A, C). The only type of glial cells that presented labeling was astrocytes. In astroglial somata, the labeling was present on similar

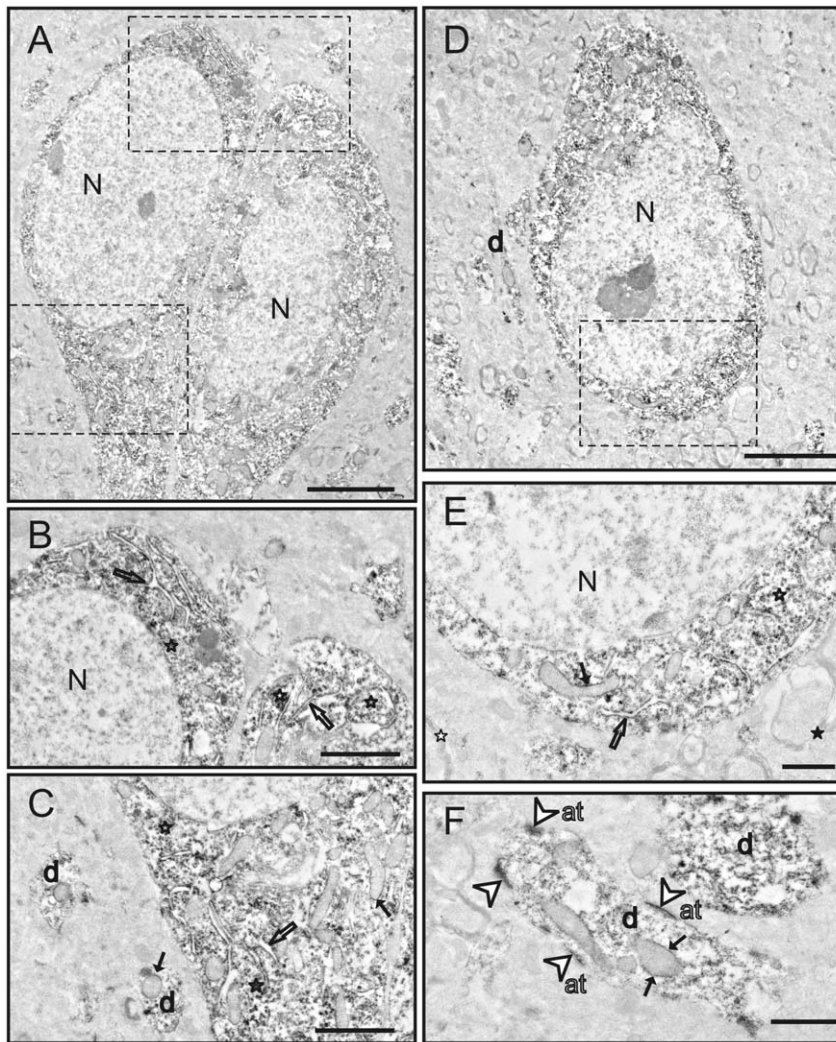


**Figure 4. Electron microscopy images of GSK3 $\beta$  labeling in the piriform cortex.** **A)** Two adjacent labeled neurons. **B)** Detail of neurons in **A** showing GSK3 $\beta$  labeling is located in the rough endoplasmic reticulum (outlined arrows) and free ribosomes (outlined stars). **C)** Detail of neurons in **A** showing labeled mitochondria (black arrows), abundant labeled free ribosomes (outlined stars), and also labeled rough endoplasmic reticulum (outlined arrows). Note also the labeling in dendrites (d). **D)** Another labeled neuron with strong cytoplasmic staining. Dendrites (d) are also labeled. **E)** Detail of neuron in **D** showing strongly labeled rough endoplasmic reticulum (outlined arrow), free ribosomes (outlined stars) and also labeling on the outer surface of the mitochondria (black arrows). Note also unlabeled myelinated axons (black star). **F)** High magnification image of two dendrites (d). GSK3 $\beta$  staining is conspicuously present on the postsynaptic density (outlined arrowheads). Cytoplasmic elements including the outer membrane of mitochondria (black arrows) are also labeled. However, no labeling is present in axon terminals (at). [N: nucleus; Scale bars: 4  $\mu$ m in A–D; 1  $\mu$ m in B–C and E–F]

doi:10.1371/journal.pone.0008911.g004

structures as in neuronal somata (Figure 5B). Labeling in small glial processes throughout the neuropil and in astrocytic end feet on capillaries was often apparent (Figure 5B–D). Thus, the examination by EM revealed the specific subcellular distribution of the GSK3 $\beta$  in the brain, which was not fully known.

#### Distribution of pSer9GSK3 $\beta$ at the Light and Electron Microscope

Although GSK3 $\beta$  is a constitutively active kinase, its activity is subject to modulation, and phosphorylation at its serine-9 residue is well recognized as one of the primary regulatory modifications [32–36]. Hence, phosphorylation of serine-9 correlates with reduced GSK3 $\beta$  activity. The goal was to examine the distribution of the latent pSer9GSK3 $\beta$  in the brain. The antibody specific for pSer9GSK3 $\beta$  (Cell Signaling, catalog #9336) was initially tested

for its specificity by immunoblot analysis. Basal pSer9GSK3 $\beta$  was clearly visible in mouse brain lysate immunoblots (Figure 6A), and treatment of mice with pilocarpine, which increases phosphorylation at serine-9 [15], resulted in a noticeable increase in pSer9GSK3 $\beta$  immunoreactivity in western-blots (Figure 6A). pSer9GSK3 $\beta$  was also blotted in parallel with the total GSK3 $\beta$  antibody to confirm that the phospho-specific antibody recognized the correct molecular weight of GSK3 $\beta$  (approximately 47 kDa), which it did (Figure 6A). Although the manufacturer of the pSer9GSK3 $\beta$  antibody, Cell Signaling, does mention the possibility of minor cross reactivity of this antibody with the phosphorylated GSK3 $\alpha$  isoform, our immunoblot analysis showed that this antibody reacts with pSer9GSK3 $\beta$  to phosphorylated GSK3 $\alpha$  at a 9.7 to 1 ratio, respectively, in an overexposed blot. Thus phospho-GSK3 $\alpha$  labeling is inconsequential. Together, these

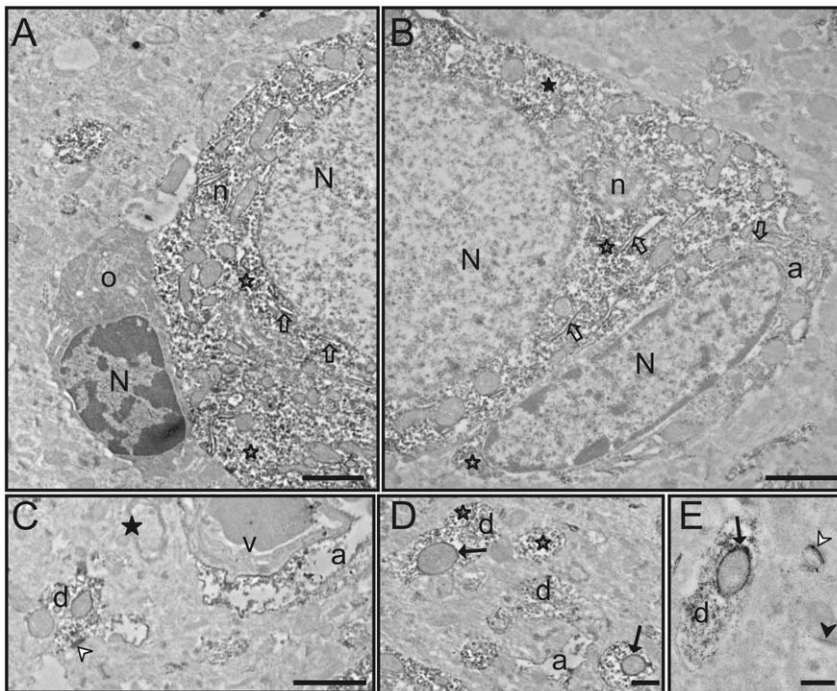


**Figure 5. Electron microscopy images of GSK3 $\beta$  labeling in the piriform cortex.** **A)** Partial image of a neuron (n) with an adjacent oligodendrocyte (o). The cytoplasm of the neuron presents abundant and strongly labeled rough endoplasmic reticulum (outlined arrows) and free ribosomes (outlined stars). In contrast, the adjacent oligodendrocyte (o) is completely devoid of immunostaining. The electron-dense appearance of the oligodendrocyte cytoplasm is not due to GSK3 $\beta$  labeling [this is the typical appearance of an unlabeled mature oligodendrocyte cytoplasm]. **B)** Image of a labeled astrocyte (a) adjacent to a labeled neuron (n). Both the small cytoplasm of the astrocyte and the abundant cytoplasm of the neuron present labeling in the rough endoplasmic reticulum (outlined arrows) and in free ribosomes (outlined stars). **C)** A labeled astrocytic process (a) is surrounding an unlabeled blood vessel (v). The basement membrane and endothelial cell are devoid of labeling. A dendrite (d) and a postsynaptic density (white arrowhead) are also labeled. Note that myelin is completely devoid of immunostaining (black star). **D)** Detail image of a GSK3 $\beta$  dendrite (d). Strongly labeled mitochondria (black arrows) and free ribosomes (outlined stars) are also seen. **E)** Examples of two synapses. One is a GSK3 $\beta$ -labeled synapse (white arrowhead), while the other synapse is unlabeled (black arrowhead). Note the rich cytoplasmic stain in the dendrite (d) and the staining of the outer mitochondrial membrane (black arrow). [N: nucleus; Scale bars: 2  $\mu$ m in A–B; 1  $\mu$ m in C–E] doi:10.1371/journal.pone.0008911.g005

findings confirmed the specificity of the pSer9GSK3 $\beta$  antibody and indicated that it could be used for the immunohistochemical analysis at the light and electron microscope.

The rostrocaudal localization of pSer9GSK3 $\beta$  immunolabeling was first analyzed at the light microscope, and then representative brain areas were selected for the subsequent analysis of subcellular distribution using electron microscopy. At the light microscope pSer9GSK3 $\beta$  was evident in the rostrocaudal extent of the brain, but compared to the phospho-independent GSK3 $\beta$ , the pSer9GSK3 $\beta$  staining pattern was markedly different and less intense with far fewer pSer9GSK3 $\beta$ -positive cells. In contrast with the phospho-independent GSK3 $\beta$  staining, the pSer9GSK3 $\beta$  staining was abundantly present in glial cells and glial processes in all brain regions. Most of the labeled glial cell bodies corresponded with non-reactive microglia cells, which also displayed pSer9GSK3 $\beta$ -labeled processes (Figures 6B–C insets, 6G–H). Labeled neurons were present in discrete areas, mostly in cortical regions and more abundantly in superficial layers of the cortex (Figure 6B–D). For example, in the motor and somatosensory cortex pSer9GSK3 $\beta$ -labeled neurons were more abundant in superficial layers (Figure 6B) and their abundance progressively diminished, with the deeper layers almost devoid of labeled neurons (Figures 6B–C). Here the immunolabeling was mainly confined to non-reactive microglia cells. pSer9GSK3 $\beta$  neuronal labeling appears mainly in the cell body, and labeling of the neuronal processes is not clearly evident (Figures 6B, 6D). In some

other cortical areas such as the piriform cortex (Figure 6D) pSer9GSK3 $\beta$ -labeled neurons are interspersed with labeled microglia cells (Figure 6D). In the hippocampus, in contrast with what was observed for GSK3 $\beta$ , pSer9GSK3 $\beta$  immunolabeling was almost exclusively observed in microglia cell bodies and glia processes (Figures 6E–H). Other brain areas presented a similar pattern of pSer9GSK3 $\beta$  labeling at the light microscope, with abundant labeling of non-reactive microglia and scarce labeling of neurons. These regions include the striatum (Figure 6C and 6C inset), the thalamus, the substantia nigra, and other midbrain and brainstem nuclei. The cerebellum presented labeling in Purkinje cells as well as abundant microglia labeling (not shown).

Due to the presence of different patterns of staining at the light microscope (i.e. regions with neuronal and glia labeling versus regions presenting almost exclusively glia staining), several representative areas of the brain were selected for closer analysis by the electron microscope, including the piriform and motor cortex, and the striatum. Overall, the subcellular localization of pSer9GSK3 $\beta$  in the immunolabeled cells was similar in all these regions with frequent presence of labeling in free ribosomes, endoplasmic reticulum, and in the nuclei of microglia and neurons (Figure 7A–E). In addition, astrocytic processes were frequently observed containing pSer9GSK3 $\beta$  labeling (Figure 7E–F). In contrast with what was observed for GSK3 $\beta$ , very scarce pSer9GSK3 $\beta$  immunolabeling was observed in mitochondria (Figure 7A, E–F). Thus, at the ultrastructural level, the distribution

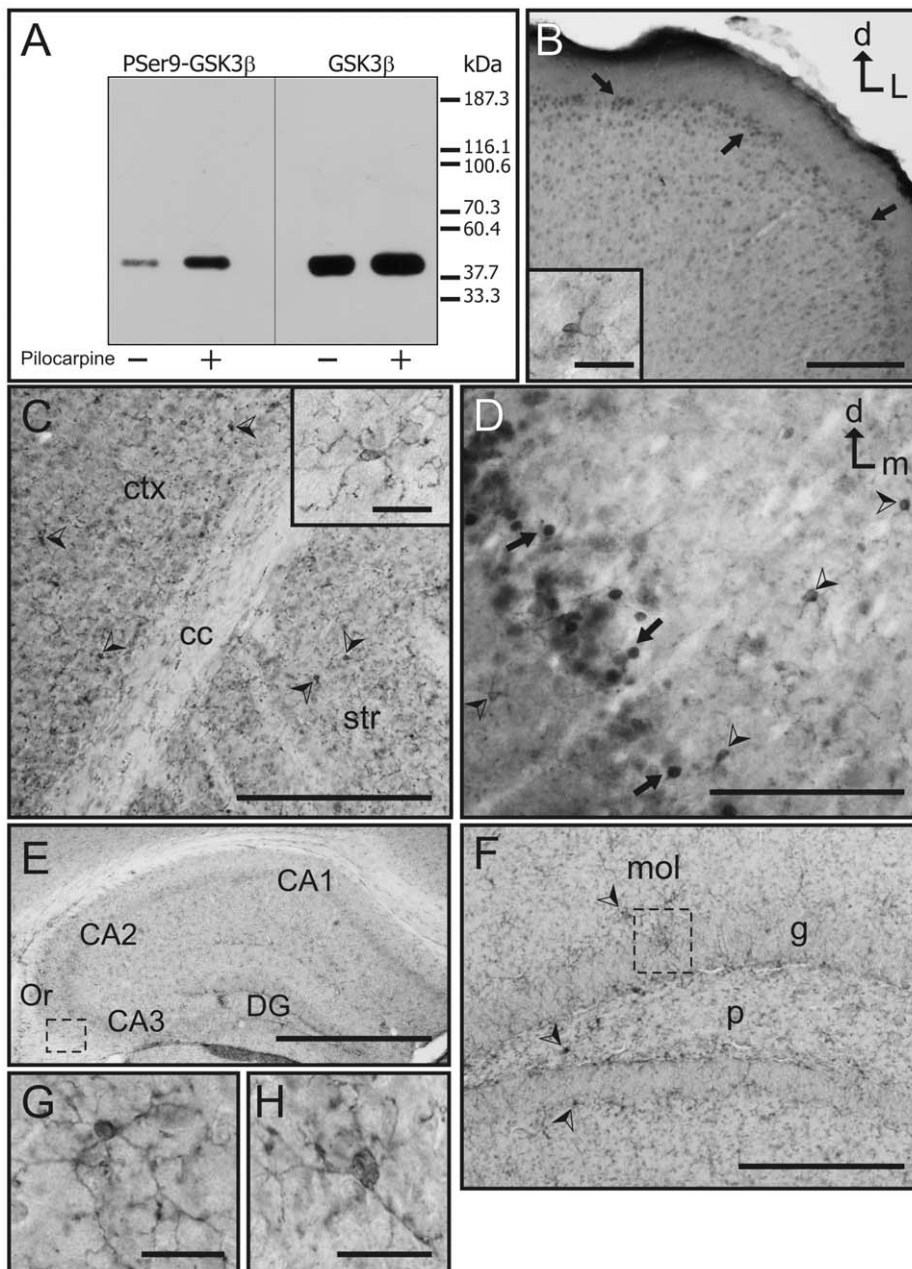


**Figure 6. Light microscopy localization of pSer9GSK3 $\beta$  in the mouse brain.** **A)** Immunoblot of mouse brain lysates showing the specificity of the pSer9GSK3 $\beta$  antibody used and its comparison with an immunoblot for GSK3 $\beta$ . For both blots, brain samples from control (–) and pilocarpine-treated (+) animals were used. Both antibodies detected only one protein band of equal molecular weight on the immunoblots. The pSer9GSK3 $\beta$  antibody detected the basal pSer9GSK3 $\beta$  and the pilocarpine-induced increase in pSer9GSK3 $\beta$ . **B)** pSer9GSK3 $\beta$  labeling in the motor cortex. Note the abundance of labeled neurons (arrows) in the superficial layers while neuronal labeling decreases progressively in deeper layers where microglia labeled cells are more frequent. **B-inset:** detail of a labeled microglia cell located in the deeper layers of the motor cortex showing staining in the cell body and processes. **C)** pSer9GSK3 $\beta$  labeling in cortical and subcortical areas. Low magnification image showing most of the labeling in microglia (arrowheads) both in the somatosensory cortex (ctx) and in the striatum (str). **C-inset:** Detail of a labeled microglia cell in the striatum showing staining in the cell body and fine processes. **D)** Image of the piriform cortex where pSer9GSK3 $\beta$  labeling is present both in neurons (arrows) and in microglia cells (arrowheads). Note that positive neurons are concentrated in one narrow strip, while microglia cells are present interspersed with labeled neurons and also in more medial and lateral areas. **E)** Low magnification image of pSer9GSK3 $\beta$  labeling in the hippocampus. All hippocampal areas present almost exclusively glial staining. The boxed area is shown as a detail in **G**. **F)** Image of pSer9GSK3 $\beta$  staining in different layers of the dentate gyrus showing immunolabeled microglial cells (arrowheads). Note the absence of immunostaining in neurons of the granule cell layer (g). The boxed area is shown in detail in **H**. **G)** Detail of a labeled microglia cell in the stratum oriens of the hippocampus showing intense immunostaining in the cell body and processes. **H)** Detail of a labeled microglia cell in the granule cell layer of the dentate gyrus showing intense immunostaining in the cell body and processes. [CA1, CA2, CA3: Cornu Amonis subfields; cc: corpus callosum; ctx: cortex; d: dorsal; DG: Dentate Gyrus; L: lateral; m: medial; mol: molecular layer of the DG; Or: stratum oriens; p: polymorphic layer of the DG. Str: striatum. **Scale bars:** 100  $\mu$ m in E; 25  $\mu$ m in B–D and F, 5  $\mu$ m in B-inset, C-inset and G–H] doi:10.1371/journal.pone.0008911.g006

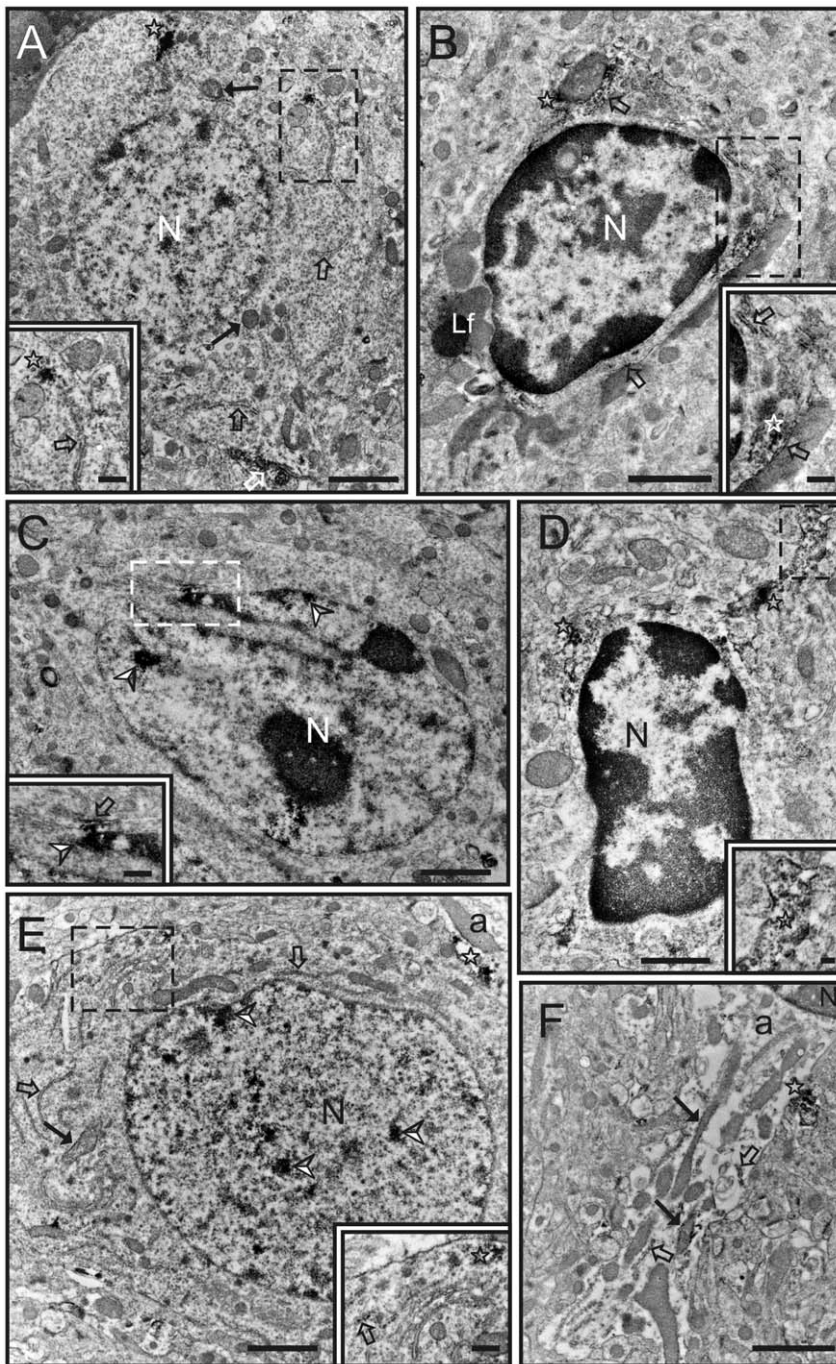


**Figure 7. Electron microscopy images of pSer9GSK3 $\beta$  labeling in cortical and subcortical areas.** **A)** pSer9GSK3 $\beta$  labeling in a neuron in the piriform cortex. The labeling is located in the rough endoplasmic reticulum (outlined arrows), free ribosomes (stars) and the outer mitochondrial membrane (black arrow). Note the strong staining in a cluster of free ribosomes in **A inset**. **B)** pSer9GSK3 $\beta$  immunolabeling in a microglia cell in the piriform cortex. Staining is present in the rough endoplasmic reticulum (outlined arrows) as well as in free ribosomes (stars). **B inset** shows a detail of the labeling present in this cell. **C)** pSer9GSK3 $\beta$  labeling in another microglia cell in the piriform cortex. In this case labeling is prominently present in the nucleus (arrowheads) while the cytoplasmic labeling is restricted to a small portion of the rough endoplasmic reticulum (outlined arrow). **C inset** shows a detail of the labeling present in the nucleus (arrowhead) and the rough endoplasmic reticulum (outlined arrow) in the proximity of the outer nuclear membrane. **D)** pSer9GSK3 $\beta$  staining in a microglia cell in the striatum. Labeling is prominent in clusters of free ribosomes (stars) in the cytoplasm as well as in the process (see **D inset**). **E)** Photomicrograph of pSer9GSK3 $\beta$  staining in a neuron in the motor cortex. Note the prominent labeling in the nucleus (arrowheads). Labeling is also present in the rough endoplasmic reticulum (outline arrows, see also **E inset**), as well as in clusters of free ribosomes and in the outer membrane of one mitochondria (black arrow). Note also the presence of an astrocytic process (a) showing immunolabeling in free ribosomes (star). **F)** Detail of an astrocytic process (a) showing pSer9GSK3 $\beta$  immunolabeling in rough endoplasmic reticulum (outlined arrow), free ribosomes (star) and mitochondria (black arrows). [Lf: Lipofuscin body; N: nucleus; Scale bars: 1  $\mu$ m in A–C, E; 0.5  $\mu$ m in D; 0.25  $\mu$ m in B inset, C inset; 0.1  $\mu$ m in D inset] doi:10.1371/journal.pone.0008911.g007

of pSer9GSK3 $\beta$  staining was highly localized and contrasted with the phospho-independent GSK3 $\beta$  staining.

## Discussion

GSK3 $\beta$  plays a diverse role in normal brain function, and its dysregulation is believed to underlie some psychiatric disorders and neurodegenerative diseases [16,37,38]. In light of the critical role of GSK3 $\beta$  in the CNS, several groups have studied the expression pattern and activity of endogenous GSK3 $\beta$  in the brain by immunohistochemistry and light microscopy during brain development, in brain disease processes, and in response to various stimuli [4,5,25–31]. In this regard the light microscopy data reported in the present study is supportive of many of the earlier reports. However, to further elucidate the distribution of GSK3 $\beta$  at the subcellular level, the expression of this kinase was also evaluated by electron microscopy. Although Hoshi et al. [39,23] originally described expression of GSK3 $\beta$  in brain mitochondria by electron microscopy, a detailed analysis of GSK3 $\beta$  expression at the ultrastructural level has not been reported previously. Thus, the main goals of this study were to corroborate the distribution of GSK3 $\beta$  in the brain, and to examine in detail the subcellular distribution of this protein.

Initial examination by light microscopy revealed that GSK3 $\beta$  is expressed in brain neurons throughout all the rostrocaudal extent of the adult mouse brain. Overall, the distribution observed in our light microscopy study mostly concurs with findings in previous studies. Takahashi et al. [25] had originally conducted an extensive immunohistochemical survey of GSK3 $\beta$  expression in the developing and adult rat cerebellum. In their study, in which GSK3 $\beta$  is referred by its other name,  $\tau$  protein kinase I, they reported GSK3 $\beta$  expression in axonal fibers of the axonal tract and in the granular layer. Expression of which they reported decreased during later stages of development [25]. They also found that GSK3 $\beta$  immunostaining in the molecular layer increased in later stages of development, and the Purkinje cells in the Purkinje cell layer had staining mainly in their cytoplasm [25]. These findings were subsequently confirmed by Leroy and Brion [28]. In our study we have found that in the mature mouse brain, the Purkinje cell layer and the molecular cell layer (where the dendritic processes of Purkinje cells end) present strong GSK3 $\beta$  labeling, while the granular cell layer was devoid of immunostaining and non-axonal staining was observed. These data are generally in accordance with previously reported studies, however Takahashi et al [25] and Leroy and Brion [28] reported some immunostaining in the granular cell layer of the adult rat brain. This discrepancy could be due to several reasons including a difference in species (mice in our study versus rats), gender (i.e. the studies in rat do not state if they have used male or female animals), or age of the animals used. In addition, it was previously reported that in the adult rat brain there was strong staining in the hippocampus in the CA and dentate gyrus regions, the deeper cortical layers, thalamic nuclei, and the substantia nigra *pars compacta* [28]. However, our findings indicated a lack of GSK3 $\beta$  staining in most hypothalamic areas of the adult mouse brain, whereas previously strong labeling of GSK3 $\beta$  was noted in this region of the brain in the adult rat [28]. This difference could also potentially reflect some variance between the two species or perhaps a gender difference. Overall, the present light microscopy data mostly concurred with previous findings on GSK3 $\beta$  localization in the brain, and was meant to establish a frame of reference for examination of GSK3 $\beta$  at the subcellular level.

GSK3 $\beta$  immunolocalization was also examined by electron microscopy to scrutinize its subcellular distribution. The most

salient feature is the abundance of GSK3 $\beta$  immunostaining in the cytosol of the neuronal soma, dendritic shaft, dendrites, and dendritic spines, but no GSK3 $\beta$  labeling was observed in axons. Within neurons GSK3 $\beta$  labeling was clearly present in the rough endoplasmic reticulum (RER), free ribosomes and in the outer membrane of mitochondria. Furthermore, we also found clear presence of GSK3 $\beta$  within astrocytes, especially on their RER, free ribosomes, mitochondria, and in astrocytic processes. In contrast, other glial types, such as the oligodendrocytes and microglia showed little evidence of GSK3 $\beta$  labeling. Although several studies have already noted GSK3 $\beta$  signaling activity in isolated astrocytes [40–42], and elevated staining of phosphoserine-9 GSK3 $\beta$  in astrocytes by light microscopy has been reported in cases of human tauopathies [43], other immunohistochemical studies [28–30], could not detect, or did not report, staining of GSK3 $\beta$  in astrocytes by light microscopy. However, our data shows that GSK3 $\beta$  labeling is clearly present in astrocytes at the electron microscope level and GSK3 $\beta$  appears in several subcellular structures such as the RER, ribosomes and mitochondria, albeit at much lower levels than in neurons.

Electron microscopy data of the intracellular distribution of GSK3 $\beta$  in neurons revealed that GSK3 $\beta$  is expressed in the mitochondrial membranes, and robust GSK3 $\beta$  labeling was found on ribosomes and the rough endoplasmic reticulum. In the mitochondria, GSK3 $\beta$  was previously reported to be resident in the mitochondrial membranes of cultured SH-SY5Y cells [24], and activated GSK3 $\beta$  is believed to regulate mitochondrial metabolic output [23,44], mitochondrial motility [45], and mitochondria-linked apoptosis signaling [46,44]. In addition, GSK3 $\beta$  signaling is known to impact protein translation through its phosphorylation of eukaryotic initiation factor 2B [47] possibly at the vicinity of the ribosomes and the RER. Increased GSK3 $\beta$  activity is also known to accentuate ER stress [48]. Thus, the strong labeling of GSK3 $\beta$  at the RER and ribosomes provides further support of its known signaling activities at these sites. In contrast to the robust staining of GSK3 $\beta$  in the endoplasmic reticulum and the mitochondria was the lack of GSK3 $\beta$  staining in brain cell nuclei under both light and electron microscopy. Previously it has been shown by immunoblot analysis that GSK3 $\beta$  is present in biochemically separated nuclear fractions of normal mouse brain [20]. However, through various pharmacological treatments and molecular methods it was determined in SH-SY5Y cells that the presence of GSK3 $\beta$  in the nucleus is transient [22], and its transit between the cytosol and the nucleus is highly dynamic [49]. Thus, when isolated brain cell nuclei from healthy brain tissues are examined “en masse” by immunoblot analysis GSK3 $\beta$  can be detected in the nucleus, but GSK3 $\beta$  staining in individual healthy neuronal nuclei by microscopy may not be readily visible. Furthermore, GSK3 $\beta$  is known to accumulate in the nucleus upon activation of apoptosis signaling [50,22]. Therefore nuclear GSK3 $\beta$  labeling in the brain may be more evident in dying neurons.

Another interesting finding was the noticeable GSK3 $\beta$  labeling of some postsynaptic densities. There is emerging evidence that GSK3 $\beta$  affects neuronal synaptic plasticity and is involved in synaptic activities [51–54]. Previously, GSK3 $\beta$  had been detected in synaptosomal fractions [51,54] and in the dendrites of cultured hippocampal neurons [53]. Peineau et al. [53] have reported that GSK3 $\beta$  mediates both N-methyl-D-aspartate receptor-dependent long-term potentiation and long-term depression. Furthermore, Zhu and colleagues [52] have shown that GSK3 $\beta$  activation can impair the synapse ultrastructure in the tetanized CA3 region of the rat hippocampus, and inhibitors of GSK3 $\beta$  can restore the synapse to its normal morphology. Our report shows that GSK3 $\beta$

is present in some postsynaptic densities while others seem to be devoid of GSK3 $\beta$ , this evidence clearly indicates that GSK3 $\beta$  is located in the synapses and also that there is some degree of specificity of GSK3 $\beta$  signaling at different synapses, which requires further exploration.

Following our findings with the phospho-independent GSK3 $\beta$  antibody, it was surprising to see a marked difference of the pSer9GSK3 $\beta$  immunolabeling. For example, cell types, such as the microglia, which showed no evidence of the phospho-independent GSK3 $\beta$  staining, presented with clear and robust pSer9GSK3 $\beta$  staining. One possibility for the discrepant labeling could be that phosphorylation at serine-9 of GSK3 $\beta$  may partially block the immunoreactivity of the phospho-independent GSK3 $\beta$  antibody, thus regions with a high concentration of pSer9GSK3 $\beta$  may appear as devoid of GSK3 $\beta$ . Nonetheless, the presence of the serine-9-phosphorylated GSK3 $\beta$  within the microglia indicates that GSK3 $\beta$  must be present within these cell types. Previously, Yuskaitis and Jope [55] reported that GSK3 $\beta$  signaling in microglia promotes the lipopolysaccharide-induced production of interleukin-6 and expression of inducible nitric oxide synthase, and regulates microglial migration, all of which can be blocked by GSK3 $\beta$  inhibitors. Our findings show that GSK3 $\beta$  signaling is resident within microglia in discrete areas on free ribosomes, the ER, and in the nuclei of some cells. However, under normal conditions GSK3 $\beta$  in resting microglia is mostly in its less activated, serine-9-phosphorylated state.

pSer9GSK3 $\beta$ -labeled neurons were also evident by light and electron microscopy, but this labeling was far less pronounced than the phospho-independent GSK3 $\beta$  labeling. The clearest pSer9GSK3 $\beta$  staining was in the superficial layers of the cortex, with diminishing staining in the deeper layers. Within the stained neurons there was pSer9GSK3 $\beta$  labeling on the ribosomes on the ER, and interestingly, inside the nuclei of some neurons. Previous findings by western blot analysis of total mouse brain homogenates [20] noted a paucity of nuclear serine-9-phosphorylated GSK3 $\beta$ , but the present results indicate that there are clear regional variations in these levels.

## References

- Woodgett JR (1990) Molecular cloning and expression of glycogen synthase kinase-3/factor A. *Embo J* 9: 2431–2438.
- Hanger DP, Hughes K, Woodgett JR, Brion JP, Anderton BH (1992) Glycogen synthase kinase-3 induces Alzheimer's disease-like phosphorylation of  $\tau$ : generation of paired helical filament epitopes and neuronal localization of the kinase. *Neurosci Lett* 147: 58–62.
- Mandelkow EM, Drewes G, Biernat J, Gustke N, Van Lint J, et al. (1992) Glycogen synthase kinase-3 and the Alzheimer-like state of microtubule-associated protein  $\tau$ . *FEBS Lett* 314: 315–321.
- Pei JJ, Braak E, Braak H, Grundke-Iqbal I, Iqbal K, et al. (1999) Distribution of active glycogen synthase kinase 3 $\beta$  (GSK-3 $\beta$ ) in brains staged for Alzheimer disease neurofibrillary changes. *J Neuropathol Exp Neurol* 58: 1010–1019.
- Pei JJ, Tanaka T, Tung YC, Braak E, Iqbal K, et al. (1997) Distribution, levels, and activity of glycogen synthase kinase-3 in the Alzheimer disease brain. *J Neuropathol Exp Neurol* 56: 70–78.
- King TD, Bijur GN, Jope RS (2001) Caspase-3 activation induced by inhibition of mitochondrial complex I is facilitated by glycogen synthase kinase-3 $\beta$  and attenuated by lithium. *Brain Res* 919: 106–114.
- Avraham E, Szargel R, Eyal A, Rott R, Engelender S (2005) Glycogen synthase kinase 3 $\beta$  modulates synphilin-1 ubiquitylation and cellular inclusion formation by SIAH: implications for proteasomal function and Lewy body formation. *J Biol Chem* 280: 42877–42886.
- Carmichael J, Sugars KL, Bao YP, Rubinsztein DC (2002) Glycogen synthase kinase-3 $\beta$  inhibitors prevent cellular polyglutamine toxicity caused by the Huntington's disease mutation. *J Biol Chem* 277: 33791–33798.
- Klein PS, Melton DA (1996) A molecular mechanism for the effect of lithium on development. *Proc Natl Acad Sci U S A* 93: 8455–8459.
- Jope RS (1999) Anti-bipolar therapy: mechanism of action of lithium. *Mol Psychiatry* 4: 117–128.
- Kozlovsky N, Belmaker RH, Agam G (2000) Low GSK-3 $\beta$  immunoreactivity in postmortem frontal cortex of schizophrenic patients. *American Journal of Psychiatry* 157: 831–833.
- Emamian ES, Hall D, Birnbaum MJ, Karayiorgou M, Gogos JA (2004) Convergent evidence for impaired AKT1–GSK3 $\beta$  signaling in schizophrenia. *Nat Genet* 36: 131–137.
- Pandey GN, Dwivedi Y, Rizavi HS, Teppen T, Gaszner GL, et al. (2009) GSK-3 $\beta$  gene expression in human postmortem brain: regional distribution, effects of age and suicide. *Neurochem Res* 34: 274–285.
- Stambolic V, Ruel L, Woodgett JR (1996) Lithium inhibits glycogen synthase kinase-3 activity and mimics wingless signalling in intact cells. *Curr Biol* 6: 1664–1668.
- De Sarno P, Bijur GN, Zmijewska AA, Li X, Jope RS (2006) In vivo regulation of GSK3 phosphorylation by cholinergic and NMDA receptors. *Neurobiol Aging* 27: 413–422.
- Jope RS, Yuskaitis CJ, Beurel E (2007) Glycogen synthase kinase-3 (GSK3): inflammation, diseases, and therapeutics. *Neurochem Res* 32: 577–595.
- Jope RS, Roh MS (2006) Glycogen synthase kinase-3 (GSK3) in psychiatric diseases and therapeutic interventions. *Curr Drug Targets* 7: 1421–1434.
- Yost C, Farr GH 3rd, Pierce SB, Ferkey DM, Chen MM, et al. (1998) GBP, an inhibitor of GSK-3, is implicated in *Xenopus* development and oncogenesis. *Cell* 93: 1031–1041.
- Thomas GM, Frame S, Goedert M, Nathke I, Polakis P, et al. (1999) A GSK3-binding peptide from FRAT1 selectively inhibits the GSK3-catalysed phosphorylation of axin and  $\beta$ -catenin. *FEBS Lett* 458: 247–251.
- Bijur GN, Jope RS (2003) Glycogen synthase kinase-3 $\beta$  is highly activated in nuclei and mitochondria. *Neuroreport* 14: 2415–2419.
- Hemmings BA, Yellowlees D, Kernohan JC, Cohen P (1981) Purification of the glycogen synthase kinase 3 from rabbit skeletal muscle. Copurification with the activating factor (FA) of the (Mg-ATP) dependent protein phosphatase. *Eur J Biochem* 119: 443–451.
- Bijur GN, Jope RS (2001) Proapoptotic stimuli induce nuclear accumulation of glycogen synthase kinase-3 $\beta$ . *J Biol Chem* 276: 37436–37442.
- Hoshi M, Takashima A, Noguchi K, Murayama M, Sato M, et al. (1996) Regulation of mitochondrial pyruvate dehydrogenase activity by  $\tau$  protein kinase

- I/glycogen synthase kinase 3 $\beta$  in brain. *Proc Natl Acad Sci U S A* 93: 2719–2723.
24. Bijur GN, Jope RS (2003) Rapid accumulation of Akt in mitochondria following phosphatidylinositol 3-kinase activation. *J Neurochem* 87: 1427–1435.
  25. Takahashi M, Tomizawa K, Kato R, Sato K, Uchida T, et al. (1994) Localization and developmental changes of  $\tau$  protein kinase I/glycogen synthase kinase-3 $\beta$  in rat brain. *J Neurochem* 63: 245–255.
  26. Shiurba RA, Ishiguro K, Takahashi M, Sato K, Spooner ET, et al. (1996) Immunocytochemistry of  $\tau$  phosphoserine 413 and  $\tau$  protein kinase I in Alzheimer pathology. *Brain Res* 737: 119–132.
  27. Leroy K, Boutajangout A, Authelat M, Woodgett JR, Anderton BH, et al. (2002) The active form of glycogen synthase kinase-3 $\beta$  is associated with granulovacuolar degeneration in neurons in Alzheimer's disease. *Acta Neuropathol* 103: 91–99.
  28. Leroy K, Brion JP (1999) Developmental expression and localization of glycogen synthase kinase-3 $\beta$  in rat brain. *J Chem Neuroanat* 16: 279–293.
  29. Lee SJ, Chung YH, Joo KM, Lim HC, Jeon GS, et al. (2006) Age-related changes in glycogen synthase kinase 3 $\beta$  (GSK3 $\beta$ ) immunoreactivity in the central nervous system of rats. *Neurosci Lett* 409: 134–139.
  30. Takahashi M, Tomizawa K, Ishiguro K (2000) Distribution of  $\tau$  protein kinase I/glycogen synthase kinase-3 $\beta$ , phosphatases 2A and 2B, and phosphorylated  $\tau$  in the developing rat brain. *Brain Res* 857: 193–206.
  31. Alimohamad H, Rajakumar N, Seah YH, Rushlow W (2005) Antipsychotics alter the protein expression levels of  $\beta$ -catenin and GSK-3 in the rat medial prefrontal cortex and striatum. *Biol Psychiatry* 57: 533–542.
  32. Cross DA, Alessi DR, Cohen P, Andjelkovich M, Hemmings BA (1995) Inhibition of glycogen synthase kinase-3 by insulin mediated by protein kinase B. *Nature* 378: 785–789.
  33. Goode N, Hughes K, Woodgett JR, Parker PJ (1992) Differential regulation of glycogen synthase kinase-3 $\beta$  by protein kinase C isotypes. *J Biol Chem* 267: 16878–16882.
  34. Sutherland C, Leighton IA, Cohen P (1993) Inactivation of glycogen synthase kinase-3 $\beta$  by phosphorylation: new kinase connections in insulin and growth-factor signalling. *Biochem J* 296 (Pt 1): 15–19.
  35. Eldar-Finkelman H, Argast GM, Foord O, Fischer EH, Krebs EG (1996) Expression and characterization of glycogen synthase kinase-3 mutants and their effect on glycogen synthase activity in intact cells. *Proc Natl Acad Sci U S A* 93: 10228–10233.
  36. Fang X, Yu SX, Lu Y, Bast RC Jr, Woodgett JR, et al. (2000) Phosphorylation and inactivation of glycogen synthase kinase 3 by protein kinase A. *Proc Natl Acad Sci U S A* 97: 11960–11965.
  37. Hernandez F, Avila J (2008) The role of glycogen synthase kinase 3 in the early stages of Alzheimer's disease. *FEBS Lett* 582: 3848–3854.
  38. Rowe MK, Wiest C, Chuang DM (2007) GSK-3 is a viable potential target for therapeutic intervention in bipolar disorder. *Neurosci Biobehav Rev* 31: 920–931.
  39. Hoshi M, Sato M, Kondo S, Takashima A, Noguchi K, et al. (1995) Different localization of  $\tau$  protein kinase I/glycogen synthase kinase-3 $\beta$  from glycogen synthase kinase-3 $\alpha$  in cerebellum mitochondria. *J Biochem* 118: 683–685.
  40. Beurel E, Jope RS (2008) Differential regulation of STAT family members by glycogen synthase kinase-3. *J Biol Chem* 283: 21934–21944.
  41. Kim SD, Yang SI, Kim HC, Shin CY, Ko KH (2007) Inhibition of GSK-3 $\beta$  mediates expression of MMP-9 through ERK1/2 activation and translocation of NF-kappaB in rat primary astrocyte. *Brain Res* 1186: 12–20.
  42. Sanchez JF, Sniderhan LF, Williamson AL, Fan S, Chakraborty-Sett S, et al. (2003) Glycogen synthase kinase 3 $\beta$ -mediated apoptosis of primary cortical astrocytes involves inhibition of nuclear factor kappaB signaling. *Mol Cell Biol* 23: 4649–4662.
  43. Ferrer I, Barrachina M, Puig B (2002) Glycogen synthase kinase-3 is associated with neuronal and glial hyperphosphorylated  $\tau$  deposits in Alzheimer's disease, Pick's disease, progressive supranuclear palsy and corticobasal degeneration. *Acta Neuropathol* 104: 583–591.
  44. King TD, Clodfelder-Miller B, Barksdale KA, Bijur GN (2008) Unregulated mitochondrial GSK3 $\beta$  activity results in NADH: ubiquinone oxidoreductase deficiency. *Neurotox Res* 14: 367–382.
  45. Chen S, Owens GC, Edelman DB (2008) Dopamine inhibits mitochondrial motility in hippocampal neurons. *PLoS One* 3: e2804.
  46. Petit-Paitel A, Brau F, Cazareth J, Chabry J (2009) Involvement of cytosolic and mitochondrial GSK-3 $\beta$  in mitochondrial dysfunction and neuronal cell death of MPTP/MPP-treated neurons. *PLoS One* 4: e5491.
  47. Proud CG (2006) Regulation of protein synthesis by insulin. *Biochem Soc Trans* 34: 213–216.
  48. Song L, De Sarno P, Jope RS (2002) Central role of glycogen synthase kinase-3 $\beta$  in endoplasmic reticulum stress-induced caspase-3 activation. *J Biol Chem* 277: 44701–44708.
  49. Meares GP, Jope RS (2007) Resolution of the nuclear localization mechanism of glycogen synthase kinase-3: functional effects in apoptosis. *J Biol Chem* 282: 16989–17001.
  50. Elyaman W, Terro F, Wong NS, Hugon J (2002) In vivo activation and nuclear translocation of phosphorylated glycogen synthase kinase-3 $\beta$  in neuronal apoptosis: links to  $\tau$  phosphorylation. *Eur J Neurosci* 15: 651–660.
  51. Hooper C, Markevich V, Plattner F, Killick R, Schofield E, et al. (2007) Glycogen synthase kinase-3 inhibition is integral to long-term potentiation. *Eur J Neurosci* 25: 81–86.
  52. Zhu LQ, Wang SH, Liu D, Yin YY, Tian Q, et al. (2007) Activation of glycogen synthase kinase-3 inhibits long-term potentiation with synapse-associated impairments. *J Neurosci* 27: 12211–12220.
  53. Peineau S, Bradley C, Taghibiglou C, Doherty A, Bortolotto ZA, et al. (2008) The role of GSK-3 in synaptic plasticity. *Br J Pharmacol* 153 Suppl 1: S428–437.
  54. Peineau S, Taghibiglou C, Bradley C, Wong TP, Liu L, et al. (2007) LTP inhibits LTD in the hippocampus via regulation of GSK3 $\beta$ . *Neuron* 53: 703–717.
  55. Yuskaitis CJ, Jope RS (2009) Glycogen synthase kinase-3 regulates microglial migration, inflammation, and inflammation-induced neurotoxicity. *Cell Signal* 21: 264–273.
  56. Hughes K, Nikolakaki E, Plyte SE, Totty NF, Woodgett JR (1993) Modulation of the glycogen synthase kinase-3 family by tyrosine phosphorylation. *Embo J* 12: 803–808.